Nanoscale

ROYAL SOCIETY OF CHEMISTRY

PAPER

View Article Online
View Journal | View Issue

Check for updates

Cite this: *Nanoscale*, 2020, **12**, 15823

Efficient full-color emitting carbon-dot-based composite phosphors by chemical dispersion†

Mingye Sun, [a] Yue Han,[a] Xi Yuan, [b] Pengtao Jing,[c] Lei Zhang,[a] Jialong Zhao [b] and Youjin Zheng*[a]

Received 11th March 2020,
Accepted 25th June 2020

DOI: 10.1039/d0nr02021d

rsc.li/nanoscale

Realizing full-color emission plays a key role in exploring the luminescence mechanisms of carbon dots (CDots) and promoting the applications of CDots in light-emitting diodes (LEDs). Herein, a synthesis strategy for full-color emitting CDots was developed through the solvothermal reaction of citric acid and urea with a constant mass ratio but varying reactant concentrations in solvent. With the reactant concentrations increasing, a dual regulation mechanism including an enhanced nucleation growth process and subsequently increased C═O/C═N-related surface states should be responsible for the photoluminescence (PL) shift of CDots from blue to red. Relying on the hydrolyzation and condensation processes of 3-aminopropyltrimethoxysilane, a simple and universal method was developed by chemically dispersing the CDots into a cross-linked silica network on the surface of SiO_2 nanoparticles to produce efficient full-color emitting SiO_2/CDot composite phosphors with considerable PL quantum yields in the range of 30–60%. It was proved that the full-color emitting SiO_2/CDot composite phosphors could be flexibly applied in packaging white LEDs, releasing pure white light at the Commission Internationale de L'Eclairage (CIE) coordinates of (0.33, 0.33) with a color rendering index (CRI) of 80.4 and a high color-rendering white light coming entirely from CDots with the CIE coordinates of (0.34, 0.36) and a CRI of 97.4, indicating promising application of the full-color emitting SiO_2/CDot composite phosphors in the LED field.

Introduction

In recent years, carbon dots (CDots) have aroused widespread concern and shown great application potential in many fields, such as light-emitting diodes (LEDs),[1–10] bioimaging,[11–14] energy storage,[15,16] photocatalysis,[17–19] and sensors,[20–23] due to their excellent luminescence properties, water solubility, good stability, nontoxicity, and low cost.[24–27] Studying the luminescence properties of CDots has always been a hot and crucial issue since the CDots were first discovered.[14,27–30] Among previous studies, full-color emission of CDots was much more attractive and showed significance in addressing the luminescence origins and promoting the optical applications of CDots.[31–34]

Recently, a variety of synthesis routes have been put forward to meet the full-color emission of CDots by adjusting the reaction methods, reaction parameters, reactants, surface functional groups, and so on.[1,3,6,10,31–33] In particular, citric acid and urea as very low-cost reactants were widely chosen for the preparation of full-color emitting CDots through a solvothermal method.[32–40] For example, Tian *et al.* obtained CDots with tunable bandgap emissions ranging from the blue to red spectrum by adjusting different solvents and their combinations in the solvothermal reaction process.[32] Sun and coworkers developed a method for synthesizing full-color emitting CDots benefiting from adjustable graphitization and surface functionalization by varying the solvothermal temperatures and ratios of citric acid to urea.[33] Zhu *et al.* synthesized the seed CDots through a solvothermal reaction of citric acid and urea, and invented a seed growth method to prepare multicolor emitting CDots with variable sizes through changing the amount of seed CDots and the reaction time.[34] In addition,

[a]*School of Physics and Electronic Engineering, Mudanjiang Normal University, Mudanjiang 157011, China. E-mail: zyjmsy@163.com*
[b]*Key Laboratory of Functional Materials Physics and Chemistry of the Ministry of Education, Jilin Normal University, Changchun 130103, China*
[c]*State Key Laboratory of Luminescence and Applications, Changchun Institute of Optics, Fine Mechanics and Physics, Chinese Academy of Sciences, Changchun 130033, China*

†Electronic supplementary information (ESI) available. See DOI: 10.1039/d0nr02021d

regulating the solvothermal reaction time of citric acid and urea could also realize the full-color emission of CDots which diverse emitting states were responsible for.[40] Moreover, we found to our surprise that full-color emission of CDots could also be realized *via* a one-step process by simply changing the reactant concentrations of citric acid and urea with a constant mass ratio in solvothermal reaction solvent.

The solid-state aggregation induced photoluminescence (PL) quenching has seriously hindered the applications of CDots in the photoelectric devices requiring solid-state luminescence, especially in LEDs.[6,7,27,31–33] Therefore, to obtain efficient PL performance of CDots in the solid state has been raising growing attention in the CDot-based LED field. For this research, many strategies have been developed, for instance, mechanically incorporating CDots in polymer matrices for fabricating CDot-based photoluminescent films or phosphors,[3,5,33,38,41–43] dispersing the CDots on the surface of starch particles, as in our previous work,[44] and within inorganic matrices or silica networks for preparing CDot-based phosphors,[7,32,45–49] and coating the CDots with a SiO_2 shell for preparing CDot/SiO_2 phosphors.[36] However, the feasibility to realize full-color emission of CDots in the solid state in most of the above strategies was not verified when they were reported.[7,44–49] Meanwhile, common mechanical dispersion into polymer matrices has become a popular and universal method to prepare full-color emitting CDot-based photoluminescent films or phosphors.[3,33,38,43] Nevertheless, simple and universal methods for preparing efficient full-color emitting CDot-based phosphors by favorable chemical dispersion are still lacking at present, in consideration of the reality that mechanical dispersion into polymer matrices generally suffers from limited loading concentration of CDots.[7]

In this work, a new strategy for full-color emitting CDots through a one-step process by changing the reactant concentrations of citric acid and urea with a constant mass ratio in solvothermal reaction solvent has been put forward. With the reactant concentrations increasing, the PL of the CDots shifted gradually from blue to red. A dual regulation mechanism including the effects of particle size and C═O/C═N-related surface states was found to be responsible for the full-color emission of CDots *via* morphology, structure, and spectroscopic characterizations. To overcome solid-state PL quenching of CDots, a simple and universal method was developed to fabricate efficient full-color emitting SiO_2/CDot composite phosphors by chemically dispersing the CDots into a cross-linking silica network on the surface of SiO_2 nanoparticles after the hydrolyzation and condensation of aminosilane. Using the full-color emitting phosphors and InGaN chips with different peak wavelengths, flexible packaging schemes for white LEDs (WLEDs) were designed, in which pure white light at the Commission Internationale de L'Eclairage (CIE) coordinates of (0.33, 0.33) with a color rendering index (CRI) of 80.4 and a high color-rendering white light with CIE coordinates of (0.34, 0.36) and CRI of 97.4 were realized, indicating significant application potential of the SiO_2/CDot composite phosphors in the LED field.

Experimental section

Materials

Citric acid (99.5%), urea (99.5%), *N*,*N*-dimethylformamide (DMF, 99.8%), petroleum ether, ethyl acetate (99.0%), and 3-aminopropyltrimethoxysilane (APTMS, 97.0%) were purchased from Aladdin Chemistry Co., Limited, China. Hydrophilic SiO_2 nanoparticles with average diameters of 15–20 nm were also purchased from Aladdin Chemistry Co., Limited, China. The InGaN chips (peak wavelengths: 365, 395, and 450 nm) were purchased from Shenzhen Looking Long Technology Co., Limited, China. Epoxy silicone resin A and B components were purchased from Ausbond (China) Co., Limited. Potato starch was purchased from the supermarket. All the chemicals and reagents were directly used after being bought without further processing.

Synthesis of full-color emitting CDots

Full-color emitting CDots were prepared by changing the reactant concentrations in the reaction solvent through a solvothermal method. Typically, citric acid and urea (mass ratio: 1 : 2) were dissolved in DMF with various concentrations of 6, 12, 20, 40, 60, 90, 120, and 240 mg mL^{-1}, corresponding to CDots A, B, C, D, E, F, G, and H, respectively. Each of the above mixed solutions (25 mL) was added into 40 mL Teflon-lined stainless-steel autoclaves. The autoclaves were transferred to an oven and kept at 160 °C for 8 h. The reaction solutions were centrifuged at 12 000 rpm for 10 min to remove agglomerated particles. The supernatants were added into excess mixed solvents of petroleum ether and ethyl acetate (volume ratio: 3 : 1), and centrifuged at 8000 rpm for 10 min to wash off residual organic molecules. In this process, the supernatants of CDots A–C were concentrated using a rotary evaporator at 50 °C before being added into petroleum ether and ethyl acetate. The dark solids were then dried in a vacuum oven at 50 °C for 24 h. The resulted CDots were kept in a vacuum oven at room temperature for further characterization.

Preparation of full-color emitting SiO_2/CDot composite phosphors

A certain amount of CDots A–H original solutions (centrifuged at 12 000 rpm for 10 min to remove agglomerated particles) and APTMS were added into the appropriate amount of DMF. Typically, 40, 30, 20, 15, 10, 8, 6, and 3 mL CDots A–H original solutions were mixed with 10 mL APTMS, respectively, and the appropriate amount of DMF was then added to form 50 mL mixed solutions under continuous stirring for 5 min. Afterwards, 3 g SiO_2 nanoparticles were added. The mixed solutions were then stirred at room temperature for 3 h. The reaction mixtures were centrifuged at 8000 rpm for 10 min to remove unbonded CDots and APTMS, and the precipitated solids were solidified in a vacuum oven at 50 °C for 24 h. Full-color emitting SiO_2/CDot composite phosphors (named phosphors A-P, B-P, C-P, D-P, E-P, F-P, G-P, and H-P) were then obtained after grinding the dried blocks. The starch/CDot

phosphors were also prepared according to the above method by just replacing the SiO_2 nanoparticles with starch powder.

Fabrication of LEDs from SiO_2/CDot composite phosphors

Epoxy silicone resin A and B components (mass ratio: 1 : 4) were mixed and mechanically vibrated for 15 min. The SiO_2/CDot composite phosphors from A-P to H-P were mixed with the transparent epoxy silicone resin with mass ratio of 1 : 1, respectively, mechanically vibrated for 5 min, and kept in a vacuum oven to remove air bubbles. The phosphors used below were the mixtures of SiO_2/CDot composite phosphors and transparent epoxy silicone resin. For the fabrication of monochromatic LEDs, the phosphors from A-P to H-P were respectively dropped on the InGaN chips (peak wavelength: 395 nm), and dried in a vacuum oven at 60 °C for 1 h and 80 °C for 6 h. For the WLEDs, three packaging schemes were available. Firstly, the InGaN chip (peak wavelength: 450 nm) was covered with the phosphor H-P, dried in a vacuum oven at 60 °C for 1 h, and then the phosphor D-P was dropped and dried in a vacuum oven at 80 °C for 8 h. The mass ratio of phosphor H-P to D-P was 1 : 3. The phosphors D-P and H-P were respectively dropped on 450 nm InGaN chips to obtain the reference LED devices. Secondly, different amounts of yellow-emitting phosphor E-P were dropped on 450 nm InGaN chips, followed by drying in a vacuum oven at 60 °C for 2 h and 80 °C for 6 h. Thirdly, a 365 nm InGaN chip was covered with phosphor H-P, dried in a vacuum oven at 60 °C for 1 h, and then the phosphor B-P were dropped and dried in a vacuum oven at 80 °C for 8 h. The mass ratio of phosphor H-P to B-P was 1 : 5. The 365 nm InGaN chips were respectively coated by phosphors B-P and H-P to obtain the reference LED devices.

Characterizations

The UV-Vis absorption spectra were recorded on a UV-2700 spectrophotometer (Shimadzu). The PL quantum yields (QYs) of CDots were measured using an Otsuka QE-2000 with an integrating sphere. The PL spectra were recorded on a Hitachi F-7000 spectrophotometer and the PL QYs of SiO_2/CDot composite phosphors were measured using this spectrophotometer with an integrating sphere. The time-resolved PL spectra were recorded on a spectrofluorometer (Horiba Jobin Yvon Fluorolog-3) with a 405 nm picosecond pulsed diode laser as the excitation source. Transmission electron microscopy (TEM) images were recorded on a Philips Technai G2 transmission electron microscope. The X-ray photoelectron spectroscopy (XPS) spectra were recorded on a Thermo Fisher Scientific ESCALAB 250Xi spectrometer with monochromatic Al Kα as the X-ray source. The Fourier transform infrared spectroscopy (FT-IR) spectra were recorded on a VERTEX 70 FT-IR spectrometer. The Raman spectra were recorded on a Horiba LabRAM HR Evolution Raman spectrometer with a laser excitation of 785 nm. The energy-dispersive X-ray spectroscope (EDX) spectra were recorded on an Oxford Instruments X-MAX. The CIE coordinates, CRI, and correlated color temperatures (CCT) of the phosphor-based LEDs were measured using a PR-705 spectra scan spectroradiometer.

Results and discussion

Realizing full-color emission is increasingly crucial to promote the optical applications of CDots.[31–34] Common citric acid and urea have attracted great interest as reactants for fabricating CDots, due to their low toxicity and cost. The solvothermal reaction of citric acid and urea has been demonstrated to be an available route to acquire full-color emitting CDots by adjusting the reaction solvents, ratios of citric acid to urea, temperatures, and time.[32–40] Here, full-color emitting CDots were prepared by a one-step solvothermal reaction of citric acid and urea (constant mass ratio) with controlled reactant concentrations in DMF. Typically, the mixtures of citric acid and urea (mass ratio: 1 : 2) were added into 25 mL DMF with controlled concentrations in the range of 6–240 mg mL^{-1}, corresponding to blue–red emitting CDots (CDots A, B, C, D, E, F, G, and H). After stirring, the mixed solutions were kept in 40 mL Teflon-lined stainless-steel autoclaves at 160 °C for 8 h. For purification, the resulted solutions were centrifuged at 12 000 rpm for 10 min to remove agglomerated particles. The supernatants were added into excess mixed solvents of petroleum ether and ethyl acetate, and centrifuged at 8000 rpm for 10 min to wash off residual organic molecules. The full-color emitting CDots were obtained by drying the dark precipitates in a vacuum oven at 50 °C for 24 h.

The optical images of the CDots A–H in DMF under room light and ultraviolet light are shown in Fig. S1,† exhibiting that the emission colors of CDots could be regulated gradually from blue to red by increasing the reactant concentrations in DMF. For further study on the full-color PL properties, the PL and UV-Vis absorption spectra of the CDots were recorded and are shown in Fig. 1a and b, respectively. As seen from Fig. 1a, the PL peaks shift from 455, 500, 535, to 650 nm, resulting in the change of emission colors from blue, blue-green, green, yellow, orange, orange-red, to red for CDots A–H with the PL QYs of 33.0%, 34.6%, 33.2%, 38.3%, 48.1%, 45.9%, 38.1%, and 35.7% in DMF (Table S1†), respectively. Fig. 1b exhibits the UV-Vis absorption spectra of CDots A–H. For blue-emitting CDots (CDots A and B), an obvious absorption band in the 320–420 nm range is observed, which should be attributed to

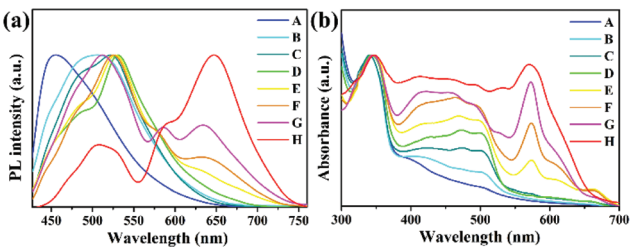

Fig. 1 (a) PL (400 nm excitation) and (b) UV-Vis absorption spectra of CDots A–H in DMF.

the n–π* transition of C═O-related surface states of CDots.[14,33,39,50–53] Meanwhile, the absorption spectra of green-emitting CDots (CDots C and D) show an apparent red shift in the range of 320–500 nm compared with blue-emitting CDots. Even more noteworthy is that another two characteristic absorption bands near 530 and 570 nm appear and gradually strengthen for CDots E–H (emission colors from yellow to red), as seen from Fig. 1b.

According to previous reports, regulating the PL wavelengths of CDots could be generally realized by two main methods, which are the effects of particle sizes (the origin is sp^2-domain sizes) and surface states induced by the functional groups of CDots.[10,21,32,33] Here, to investigate the influences of reactant concentrations on the full-color emission of CDots, three representative CDots A, D, and H were selected for further research, with typical blue, green, and red emissions. Fig. 2a–c show the TEM images of CDots A, D, and H, exhibiting that the three CDots possess spherical morphology and relatively monodisperse sizes. The high-resolution TEM (HRTEM) images in the insets of Fig. 2a–c indicate that the three CDots have similar lattice fringes with an interplanar spacing of 0.21 nm, which are assigned to the (100) plane of graphitic carbon.[4,21,32] Meanwhile, the particle sizes of CDots A are about 3.7 nm, obviously less than those of CDots D and H, which have almost similar sizes close to 5.0 nm, as shown in Fig. 2d–f. The TEM results suggest that the full-color emission of the resulted CDots is possibly related to different regulation mechanisms. Meanwhile, the mechanisms of the synthesis strategy for full-color emitting CDots by adjusting the reactant concentrations in reaction solvent have become complicated.

To address these queries, some spectroscopy measurements were carried out as shown in Fig. 2g–i. As seen from Fig. 2g, the Raman spectra of the three CDots show two characteristic peaks of D and G bands at around 1350 and 1570 cm^{-1}, due to disordered carbon structures or defects and graphite carbon structures, respectively.[33,52,54] The intensity ratios of I_D/I_G between D and G bands decrease from 0.99 to 0.80 and then increase to 1.02 for CDots A, D, and H. The decreased I_D/I_G is associated with increased graphitization degree or sp^2 domain sizes, agreeing well with the increased particle sizes, which should be responsible for the red-shifted PL from CDots A to D.[33] Meanwhile, the increased I_D/I_G suggests that the red-shifted PL of CDots H relative to CDots D is closely related to disordered carbon structures or defects on the surface of CDots, in consideration of their similar particle sizes.[52] The FT-IR spectra in Fig. 2h exhibit that the CDots possess abundant surface functional groups, including stretching vibrations of O–H (3409 cm^{-1}), N–H (3205 cm^{-1}), C–H (2940 and 2878 cm^{-1}), C═O (1719 cm^{-1}), C═N (1662 cm^{-1}), and C═C (1605 cm^{-1}), demonstrating the formation of aromatic structures containing C═O and C═N-related groups in CDots resulted from the dehydration reaction of citric acid and urea during the solvothermal process.[6,14,33,51,52] According to previous reports, abundant surface functional groups containing C═O/C═N could red-shift the PL of CDots besides particle size effects.[14,33,39,50–53] Therefore, for more precise surface chemical composition and valence state analyses, XPS spectra of the three CDots were recorded as shown in Fig. 2i. The three CDots all contain C, N, and O elemental components, with typical binding energy peaks at 285.0, 400.0, and 532.0 eV, attributed to C 1s, N 1s, and O 1s, respectively.[31,32] Table S2† lists the relative atomic concentrations of C, N, and O elemental components and their ratios to C content from the XPS spectra. The relative ratios of N to C atoms decrease from 20.6% to 7.7% for CDots A and D. Meanwhile, the O to C ratio is 31.1% in CDots A, and it reduces to 25.8% for CDots D. In addition, the ratios of N and O to C for CDots D and H increase from 7.7% and 25.8% to 13.1% and 32.3%, respectively. High-resolution N 1s and O 1s XPS spectra of the three CDots are further exhibited in Fig. 3. N 1s can be fitted with three peaks as seen from Fig. 3a–c, including pyridinic N (C═N–C, 398.9 eV), pyrrolic N (C_2–NH, 399.8 eV), and graphitic N (N–C_3, 401.7 eV).[6,31,33,54] The ratios of graphitic N to C decrease from CDots A to H. While, the relative contents of

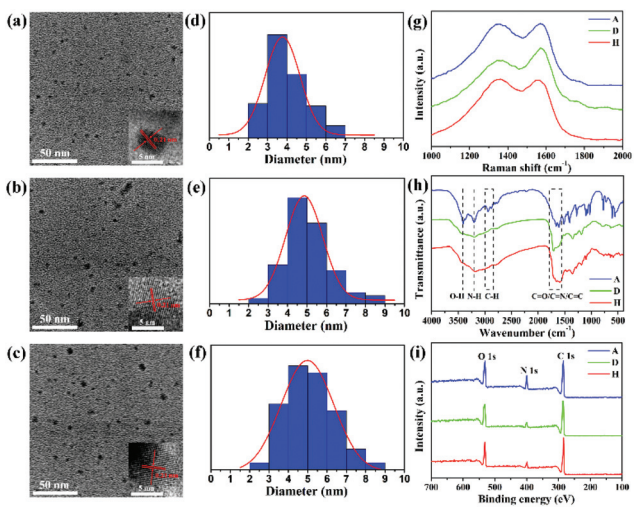

Fig. 2 (a–c) TEM images and (d–f) particle size distributions of CDots (a and d) A, (b and e) D, and (c and f) H, insets in the bottom right corners of (a–c): HRTEM images of corresponding CDots A, D, and H. (g) Raman, (h) FT-IR, and (i) XPS spectra of CDots A, D, and H.

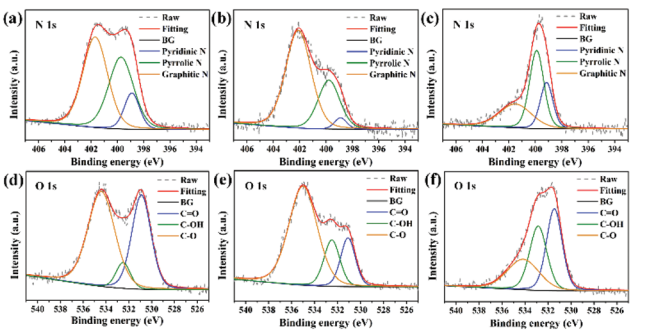

Fig. 3 High-resolution (a–c) N 1s and (d–f) O 1s XPS spectra of CDots (a and d) A, (b and e) D, and (c and f) H. "BG" stands for background line.

Table 1 Ratios of pyridinic N, pyrrolic N, graphitic N, C=O, C–OH, and C–O to C contents in CDots A, D, and H

	Ratios of each content to C (%)					
Sample	Pyridinic N	Pyrrolic N	Graphitic N	C=O	C–OH	C–O
A	2.5	8.0	10.1	11.9	2.4	16.8
D	0.3	2.2	5.2	4.3	4.5	17.0
H	3.1	5.9	4.1	12.3	10.7	9.3

pyridinic N to C reduce from CDots A to D, they exhibit an obvious increase from CDots D to H, as seen from Table 1. O 1s can be resolved into three components including C=O (531.2 eV), C–OH (532.5 eV), and C–O (534.5 eV), as shown in Fig. 3d–f.[14] The ratios of O in C=O to C decrease from CDots A to D, and then an increase is observed from CDots D to H (Table 1). All the above results indicate that the red-shifted PL of CDots D results from larger particle size relative to CDots A, rather than the changes in surface functional groups. In addition, the increases of N in C=N and O in C=O contents should be the origin of red-shifted PL for CDots H in consideration of the similar particle sizes of CDots D and H, as previous reports have suggested.[14,33,39,50–53]

The TEM, Raman, FT-IR, and XPS results of the CDots are extremely consistent with their optical properties. The CDots A, D, and H possess their own characteristic PL bands locating at 455, 535, 585 and 650 nm, respectively, as displayed in Fig. 1a. For blue-emitting CDots A, the emission band at 455 nm can be effectively excited at the excitation range from 350 to 400 nm with almost no shift in the PL peak wavelength, and the emission reaches the maximum under 390 nm excitation, as exhibited in Fig. S2a.† Meanwhile, an obvious peak shift from 455 to 500 nm and intensity weakness appear when the excitation wavelength is beyond 400 nm. These results indicate that the PL band at 455 nm for blue-emitting CDots A comes from the absorption band in the 350–400 nm range (Fig. 1b), benefiting from the n–π* transition of C=O-related surface states.[14,33,39,50–53] The PL spectra move from blue to green wavelength ranges (from 455, 500 to 535 nm) step by step for CDots A–D along with red-shifted absorption spectra in the range of 320–500 nm as shown in Fig. 1a and b, attributed to the effect of increased particle sizes.[1,10,32,33] Moreover, almost no peak wavelength shift is observed for the dominant PL band at 535 nm for green-emitting CDots D with the excitation wavelengths varying, as seen from Fig. S2b.† Meanwhile, an optimized excitation range from 400 to 500 nm is clearly detected (Fig. S2b†), matching well with the red-shifted absorption band of green-emitting CDots D relative to blue-emitting CDots A (Fig. 1b). The emerging PL bands at 585 and 650 nm should be responsible for yellow and red emissions of CDots E–H (Fig. 1a). The PL bands at 585 and 650 nm of red-emitting CDots H also exhibit excitation wavelength independence under the excitation range from 400 to 570 nm with the most preferred excitation wavelength at 530 nm as seen from Fig. S2c.† Therefore, the emerging PL bands at 585 and 650 nm should be attributed to the new characteristic absorption bands near 530 and 570 nm (Fig. 1b) assigned to increased n–π* transitions of C=O and C=N-related surface states, respectively, for CDots H relative to CDots D.[33,39,40,50–53] The typical green emission band at 535 nm is also detected in CDots H at excitation wavelengths ranging from 400 to 500 nm. Fig. S3† shows the time-resolved PL spectra of CDots A at 455 nm, CDots D at 535 nm, and CDots H at 585 and 650 nm. After being fitted, the average PL lifetimes of them are different and estimated to be 4.05, 9.59 12.47, and 12.88 ns as listed in Table S3,† respectively, verifying that the multicolor PL bands should belong to diverse state transitions.[6,40,50,53]

All these signs demonstrate that these CDots have multi-state PL and absorption features. The blue PL band at 455 nm comes from the absorption band in the range of 350–400 nm, attributed to the n–π* transition of C=O-related surface states of CDots. The green PL band at 535 nm is aligned with the red-shifted absorption band ranging from 400 to 500 nm, due to larger particle sizes of green-emitting CDots compared with blue-emitting CDots. Meanwhile, the yellow and red PL bands at 585 and 650 nm are attributed to the emerging characteristic absorption bands near 530 and 570 nm, resulted from the reduced band gap width induced by increased C=O and C=N-related surface states for red-emitting CDots relative to green-emitting CDots.[39,40,50,52,53] Therefore, the possible mechanisms of the synthesis strategy for full-color emitting CDots by simply changing the reactant concentrations in DMF should be clarified as illustrated in Scheme 1. The growth process of CDots will end as the amounts of reactants are below the nucleation growth concentration. Therefore, low reactant concentrations result in the blue-emitting CDots with smaller particle sizes. Afterwards, the CDots can grow larger in sizes with the reactant concentrations increasing, leading to a red shift in absorption and PL spectra. Meanwhile, excess reactants can no longer make contribution to the nucleation growth of CDots, but can enhance the surface oxidation and

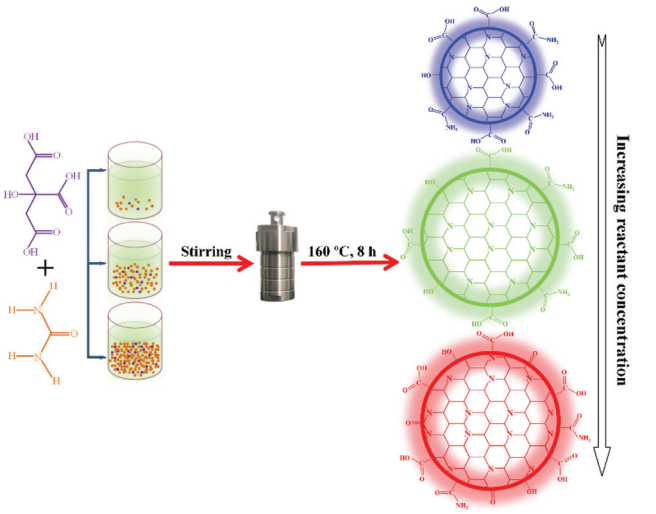

Scheme 1 Possible synthesis mechanisms for full-color emitting CDots.

nitridation of CDots, resulting in more surface functional groups containing C═O and C═N for red emission.

The surfaces of CDots are rich in functional radicals such as carboxyl, hydroxyl, and amino.[19,20,27] Hydrophilic nanosilica with low cost and nontoxicity should be an ideal dispersion matrix to prevent the solid-state PL quenching of CDots.[55] Meanwhile, there is no report as yet about direct dispersion of the CDots on the surface of SiO_2 nanoparticles through hydrogen bonding to restrain the solid-state PL quenching of CDots. For this, 15 mL CDots D original solution and 3 g hydrophilic SiO_2 nanoparticles were added into 35 mL DMF with stirring for 24 h to form SiO_2/CDot powders after centrifugation, drying, and grinding processes. Nevertheless, the SiO_2/CDot powders exhibit a weak green emission as seen in Fig. S4a and b.† Fig. S4c† shows the FT-IR spectra of the SiO_2/CDot powders, SiO_2 nanoparticles, and CDots D, illustrating that the amount of CDots D bonded on SiO_2 nanoparticles through hydrogen bonding are definitely slight. Therefore, the aminosilane coupling agent could be an extremely suitable intermediary for chemically dispersing the CDots on SiO_2 nanoparticles through amide bonds to suppress the solid-state PL quenching of CDots.[7,48,55] Here, a simple and universal preparation strategy for full-color emitting SiO_2/CDot composite phosphors was put forward. Typically, a controlled amount of full-color emitting CDots A–H original solutions, 10 mL APTMS, and 3 g SiO_2 nanoparticles were simply added into the appropriate amount of DMF to form 50 mL mixed solutions with mechanical stirring for 3 h. After centrifugation, solidifying, and grinding processes, efficient full-color emitting SiO_2/CDot composite phosphors (named phosphors A-P, B-P, C-P, D-P, E-P, F-P, G-P, and H-P) were obtained with the structure of bonded CDots into cross-linked silica network on the surface of SiO_2 nanoparticles after the hydrolyzation and condensation of APTMS. The possible formation mechanisms of the SiO_2/CDot composite phosphors are illustrated in Scheme 2.

The inset in Fig. 4a exhibits the optical images of the resulted full-color emitting SiO_2/CDot composite phosphors under room light and ultraviolet light. As seen in the inset, the emissions are strong and a gradual red shift from blue to red is observed from phosphors A-P to H-P. Fig. 4a shows the PL spectra of the phosphors at 400 nm excitation. The PL spectra

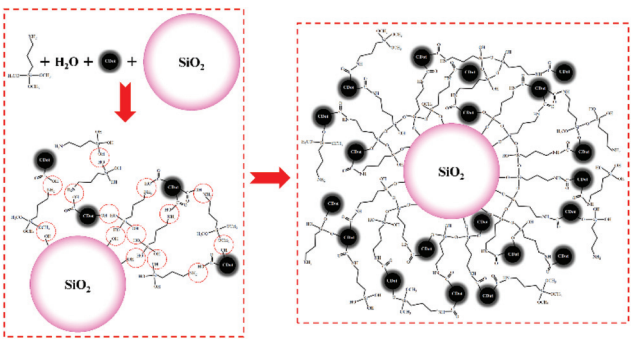

Scheme 2 Possible formation mechanisms of the SiO_2/CDot composite phosphors by chemical dispersion.

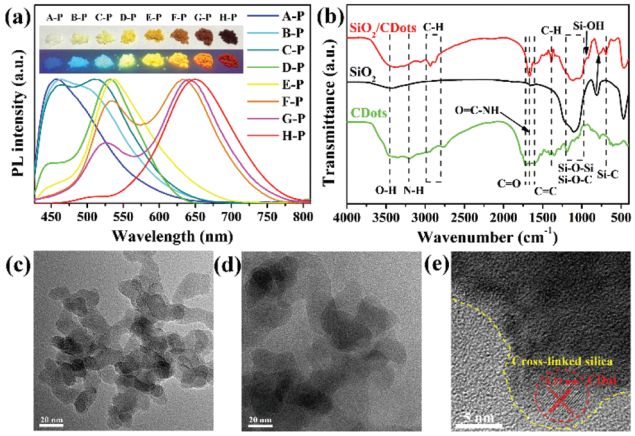

Fig. 4 (a) PL spectra of full-color emitting SiO_2/CDot composite phosphors at 400 nm excitation (inset: optical images of the SiO_2/CDot composite phosphors under room light and ultraviolet light of 365 nm). (b) FT-IR spectra of SiO_2/CDot composite phosphor D-P, SiO_2 nanoparticles, and CDot D. TEM images of (c) SiO_2 nanoparticles and (d) SiO_2/CDot composites. (e) HRTEM image of SiO_2/CDot composites.

of the CDots in solid phosphors are almost similar to those in solutions, indicating that the building process of the SiO_2/CDot composite structure *via* APTMS has almost no impact on the PL properties of CDots. Meanwhile, the PL peaks at the short wavelength range of CDots become significantly weak in the phosphors F-P–H-P possessing two major emission bands at 535 and 650 nm (Fig. 1a and 4a), attributed to the self-absorption of closer CDots in the solid state probably in consideration of the preferred excitation wavelength at 530 nm for the PL band at 650 nm (Fig. S2c†).[44] The PL QYs of the SiO_2/CDot composite phosphors are in the range of 30–60%, superior to those of the corresponding CDots in solutions as shown in Tables S1 and S4† (except for the red-emitting phosphor H-P), which should be attributed to favorable chemical dispersion of CDots. In addition, the time-resolved PL spectra of the CDots A, D, and H under different conditions were recorded, including in DMF, DMF mixed with APTMS, and SiO_2/CDot composite phosphors, as shown in Fig. S5.† The average PL lifetimes of CDots A and D vary slightly under the three conditions, but the PL dynamic processes of CDots H have become obviously fast after surface modification with APTMS, as shown in Fig. S5 and Table S5,† irrespective of whether in solution or solid state, indicating that the red PL band at 650 nm of CDots H originating from the n–π^* transition of C═N-related surface states could possibly be affected partly by surface modification, leading to the only sample with reduced PL QY for phosphors H-P (Tables S1 and S4†).

To explore the structure of the SiO_2/CDot composite phosphors, various characterization studies were carried out such as TEM, FT-IR, and XPS. The SiO_2 nanoparticles have a uniform particle size distribution in the range of 15–20 nm, as seen from Fig. 4c. Compared with pure SiO_2 nanoparticles, the sizes of the SiO_2/CDot composites obviously grow up to about 25–40 nm with the boundary between each other blurring, as

shown in Fig. 4d, indicating that a cross-linked network silica layer is formed around SiO_2 nanoparticles due to the hydrolyzation and complicated condensation processes of APTMS.[7,46,56–58] Fig. 4e shows the HRTEM image of the SiO_2/CDot composites, showing that CDots are bonded into the cross-linked silica network. The FT-IR spectra further provide credible proofs consistent with the TEM results. As seen from the FT-IR spectrum of SiO_2/CDot composite phosphor D-P compared with those of SiO_2 nanoparticles and CDot D in Fig. 4b, the three obvious absorption peaks at 2934, 2876, and 1389 cm^{-1} correspond to the antisymmetric stretching, symmetrical stretching, and bending vibrations of C–H,[14,35,46,56] and the emerging stretching vibration of the Si–C bond (701 cm^{-1}) also appears,[42,48] ensuring the presence of APTMS in the SiO_2/CDot composite phosphors. The peak at 1605 cm^{-1} for the stretching vibration of C=C verifies the content of CDots in the phosphors.[1,14,33] Notably, a significant increase in the peak ratio of 1667 to 1719 cm^{-1} is observed due to the transformation from C=O stretching vibration in COOH of CDots to CONH, suggesting the bonding of CDots with APTMS through CONH.[7,42,48,55] Moreover, some changes in the Si–O–Si vibrations in SiO_2/CDot composite phosphors emerge compared with SiO_2 nanoparticles, for example, a new peak at 1020 cm^{-1} for antisymmetric stretching vibration of Si–O–Si is observed and the symmetrical stretching vibration peak of Si–O–Si shifts from 805 to 783 cm^{-1}, indicating the formation of fresh Si–O–Si due to the coupling of APTMS on SiO_2 nanoparticles accompanied by a certain crosslinking between APTMS molecules after the hydrolyzation of APTMS with the trace amount of water in the CDot original solutions,[7,42,46,48,56] which are consistent with the TEM morphology. The increased bending vibration of S–OH at 924 cm^{-1} further confirms the hydrolyzation of APTMS.[7,46] These results uniformly demonstrate that the CDots are chemically dispersed into a cross-linked silica network on the surface of SiO_2 nanoparticles through CONH after the hydrolyzation and complicated condensation processes of APTMS, as displayed in Scheme 2. Fig. S6† displays the XPS full spectra of the SiO_2/CDot composite phosphor D-P, SiO_2 nanoparticles, and CDot D, showing that the SiO_2/CDot composite phosphors contain C, N, O, and Si elements. The relative atomic concentrations of SiO_2/CDot composite phosphors and SiO_2 nanoparticles are listed in Table S6,† as evaluated by EDX (Fig. S7†). The high-resolution Si 2p and O 1s XPS spectra of SiO_2 nanoparticles are shown in Fig. S8a and b.† Fig. S8c and d† exhibit the high-resolution Si 2p and C 1s XPS spectra of the SiO_2/CDot composite phosphors. It can be seen that the XPS results are basically consistent with the FT-IR data. In addition, the starch/CDot phosphors were also prepared *via* this method by just replacing the SiO_2 nanoparticles with starch powder, as shown in Fig. S9,† demonstrating great flexibility of this preparation strategy for full-color emitting CDot-based phosphors.

Benefiting from the merits of high PL QYs and full-color emission, the SiO_2/CDot composite phosphors have great application potential in LEDs. Fig. 5 shows the optical images and emission spectra of monochromatic LEDs from blue to red (named A-L1, B-L1, C-L1, D-L1, E-L1, F-L1, G-L1, and H-L1), prepared by depositing the mixtures of full-color emitting SiO_2/CDot composite phosphors and epoxy silicone resin on commercial InGaN chips with the peak wavelength at 395 nm. The monochromatic LEDs exhibit the characteristic emission colors of corresponding SiO_2/CDot composite phosphors from blue, green, to red, with emission peaks from 455, 540, to 685 nm. The emission spectra of the CDots in LEDs exhibit a red shift relative to those of SiO_2/CDot composite phosphors, as seen from Fig. 4a and 5, attributed to enhanced self-absorption for the emitted light of CDots in the propagation process from the inside of InGaN chips to the outside.

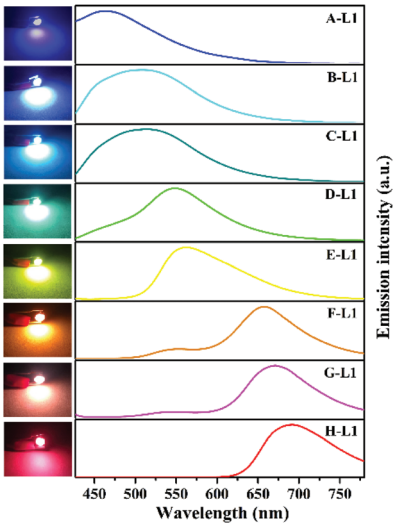

Fig. 5 Optical images and emission spectra (under 3.0 V) of the monochromatic LEDs (A-L1–H-L1) fabricated from full-color emitting SiO_2/CDot composite phosphors (A-P–H-P).

For the fabrication of WLEDs, the phosphors H-P and D-P mixed with epoxy silicone resin were successively deposited on a 450 nm InGaN chip to prepare the WLED device named W-L2. Fig. 6a and b show the optical images of the colored pens under room light and the W-L2. The emission spectrum of the W-L2 was measured under 3.0 V as shown in Fig. 6f, along with the emission spectra of reference devices based on phosphors D-P and H-P, named D-L2 and H-L2, respectively. The CIE coordinates of W-L2 are (0.33, 0.33), indicating extremely pure white light with a CRI of 80.4 and a CCT of 5381 K, as seen from the CIE chromaticity chart in Fig. 6d. In view of the broad PL spectrum of yellow-emitting CDot E, the phosphor E-P with three increasing amounts was respectively dropped on the InGaN chips with the emission peak at 450 nm for the WLEDs (named E-L2-1, E-L2-2, and E-L2-3). Fig. S10a and b† display their CIE coordinates and emission spectra. Nevertheless, the white light emissions of the above WLEDs assuredly rely on the blue light from the basal InGaN chips. Therefore, based on the 365 nm InGaN chip, the blue-green and red-emitting phosphor B-P and H-P were selected to prepare the WLED device (named W-L3), in which white light was emitted absolutely from the SiO_2/CDot composite phos-

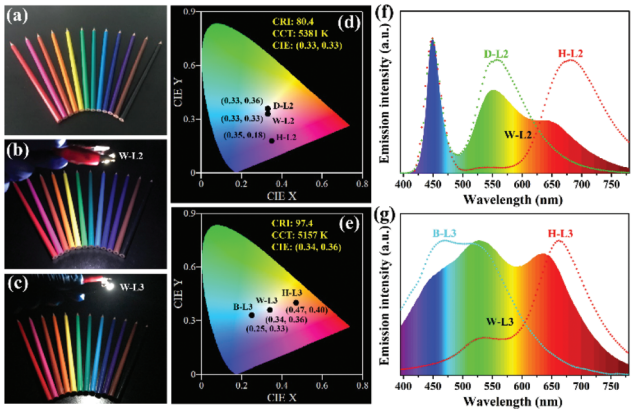

Fig. 6 Optical images of the colored pens under (a) room light, (b) W-L2, and (c) W-L3. (d and e) CIE chromaticity charts and (f and g) emission spectra (under 3.0 V) of (d and f) W-L2, (e and g) W-L3, and reference devices (D-L2 and H-L2 based on phosphors D-P and H-P *via* 450 nm InGaN chips, B-L3 and H-L3 based on phosphors B-P and H-P *via* 365 nm InGaN chips, respectively).

phors. Fig. 6c shows the optical image of colored pens under the WLED device W-L3. Fig. 6g shows the emission spectra of the W-L3 and reference devices (B-L3 and H-L3, based on phosphors B-P and H-P, respectively) under 3.0 V, indicating the full spectrum coverage in the visible-light range from 400 to 760 nm for the W-L3 as compared with the sunlight spectrum in Fig. S11.† As a result, white light with an excellent CRI of 97.4 and CIE coordinates of (0.34, 0.36) is realized (Fig. 6e). These results prove significant application potential of the full-color emitting SiO_2/CDot composite phosphors in the LED field.

Conclusions

In conclusion, we have put forward a new synthesis strategy for full-color emitting CDots through a one-step solvothermal reaction of citric acid and urea with constant mass ratio by simply altering the reactant concentrations in DMF. The nucleation growth became intensive meaning larger particle sizes of CDots with the reactant concentrations increasing, leading to the shift for the PL spectra of CDots from blue to green. Meanwhile, excess reactants could no longer make a contribution to the nucleation growth of CDots, but could promote the generation of C═O and C═N-related surface states, which was responsible for further PL shift of CDots from green to red. To suppress the solid-state PL quenching of CDots, a simple and universal method was developed *via* chemically dispersing CDots into a cross-linked silica network on the surface of SiO_2 nanoparticles after the hydrolyzation and condensation processes of APTMS for efficient full-color emitting SiO_2/CDot composite phosphors with considerable PL QYs in the range of 30–60%. Flexible packaging schemes were designed for WLEDs based on the full-color emitting SiO_2/CDot composite phosphors, representatively including a pure white light at the CIE coordinates of (0.33, 0.33) with a CRI of 80.4 and a high color-rendering white light coming entirely from CDots at the CIE coordinates of (0.34, 0.36) with a CRI of 97.4, indicating significant application potential of the full-color emitting SiO_2/CDot composite phosphors in the LED field. We anticipate that this work could develop a new route for the preparation of full-color emitting CDot-based luminescent materials.

Conflicts of interest

There are no conflicts to declare.

Acknowledgements

This work was supported by the University Nursing Program for Young Scholars with Creative Talents in Heilongjiang Province (no. UNPYSCT-2017196), the Cultivating Project for Outstanding Young Scholars of Mudanjiang Normal University (no. QC2017001), the Scientific Research Starting Fund for Doctor of Mudanjiang Normal University (no. MNUB201508), and the Scientific Research Project of Education Department of Heilongjiang Province (no. 1351SMYYB011).

Notes and references

1 F. Yuan, Z. Wang, X. Li, Y. Li, Z. Tan, L. Fan and S. Yang, *Adv. Mater.*, 2017, **29**, 1604436.
2 Y. Zhang, P. Zhuo, H. Yin, Y. Fan, J. Zhang, X. Liu and Z. Chen, *ACS Appl. Mater. Interfaces*, 2019, **11**, 24395–24403.
3 Z. Wang, F. Yuan, X. Li, Y. Li, H. Zhong, L. Fan and S. Yang, *Adv. Mater.*, 2017, **29**, 1702910.
4 Y. Chen, M. Zheng, Y. Xiao, H. Dong, H. Zhang, J. Zhuang, H. Hu, B. Lei and Y. Liu, *Adv. Mater.*, 2016, **28**, 312–318.
5 W. Kwon, S. Do, J. Lee, S. Hwang, J. K. Kim and S. Rhee, *Chem. Mater.*, 2013, **25**, 1893–1899.
6 T. Feng, Q. Zeng, S. Lu, X. Yan, J. Liu, S. Tao, M. Yang and B. Yang, *ACS Photonics*, 2018, **5**, 502–510.
7 Y. Zhan, B. Shang, M. Chen and L. Wu, *Small*, 2019, **15**, 1901161.
8 X. Zhang, Y. Zhang, Y. Wang, S. Kalytchuk, S. V. Kershaw, Y. Wang, P. Wang, T. Zhang, Y. Zhao, H. Zhang, T. Cui, Y. Wang, J. Zhao, W. W. Yu and A. L. Rogach, *ACS Nano*, 2013, **7**, 11234–11241.
9 H. Choi, S. Ko, Y. Choi, P. Joo, T. Kim, B. R. Lee, J. Jung, H. J. Choi, M. Cha, J. Jeong, I. Hwang, M. H. Song, B. Kim and J. Y. Kim, *Nat. Photonics*, 2013, **7**, 732–738.
10 F. Yuan, T. Yuan, L. Sui, Z. Wang, Z. Xi, Y. Li, X. Li, L. Fan, Z. Tan, A. Chen, M. Jin and S. Yang, *Nat. Commun.*, 2018, **9**, 2249.
11 S. Yang, L. Cao, P. G. Luo, F. Lu, X. Wang, H. Wang, M. J. Meziani, Y. Liu, G. Qi and Y. Sun, *J. Am. Chem. Soc.*, 2009, **131**, 11308–11309.

12 M. Zheng, S. Liu, J. Li, D. Qu, H. Zhao, X. Guan, X. Hu, Z. Xie, X. Jing and Z. Sun, *Adv. Mater.*, 2014, **26**, 3554–3560.
13 K. Jiang, S. Sun, L. Zhang, Y. Lu, A. Wu, C. Cai and H. Lin, *Angew. Chem., Int. Ed.*, 2015, **54**, 5360–5363.
14 W. Li, S. Wu, H. Zhang, X. Zhang, J. Zhuang, C. Hu, Y. Liu, B. Lei, L. Ma and X. Wang, *Adv. Funct. Mater.*, 2018, **28**, 1804004.
15 V. C. Hoang, K. Dave and V. G. Gomes, *Nano Energy*, 2019, **66**, 104093.
16 D. Chao, C. Zhu, X. Xia, J. Liu, X. Zhang, J. Wang, P. Liang, J. Lin, H. Zhang, Z. X. Shen and H. J. Fan, *Nano Lett.*, 2015, **15**, 565–573.
17 J. Liu, Y. Liu, N. Liu, Y. Han, X. Zhang, H. Huang, Y. Lifshitz, S. Lee, J. Zhong and Z. Kang, *Science*, 2015, **347**, 970–974.
18 H. Yu, R. Shi, Y. Zhao, G. I. N. Waterhouse, L. Wu, C. Tung and T. Zhang, *Adv. Mater.*, 2016, **28**, 9454–9477.
19 Y. Liu, X. Li, Q. Zhang, W. Li, Y. Xie, H. Liu, L. Shang, Z. Liu, Z. Chen, L. Gu, Z. Tang, T. Zhang and S. Lu, *Angew. Chem., Int. Ed.*, 2020, **59**, 1718–1726.
20 H. Wu, Y. Chen, X. Dai, P. Li, J. F. Stoddart and Y. Liu, *J. Am. Chem. Soc.*, 2019, **141**, 6583–6591.
21 S. Lu, G. Xiao, L. Sui, T. Feng, X. Yong, S. Zhu, B. Li, Z. Liu, B. Zou, M. Jin, J. S. Tse, H. Yan and B. Yang, *Angew. Chem., Int. Ed.*, 2017, **56**, 6187–6191.
22 K. Jiang, Y. Wang, C. Cai and H. Lin, *Adv. Mater.*, 2018, **30**, 1800783.
23 F. Zhao, T. Zhang, Q. Liu and C. Lü, *Sens. Actuators, B*, 2020, **304**, 127344.
24 Y. Sun, B. Zhou, Y. Lin, W. Wang, K. A. S. Fernando, P. Pathak, M. J. Meziani, B. A. Harruff, X. Wang, H. Wang, P. G. Luo, H. Yang, M. E. Kose, B. Chen, L. M. Veca and S. Xie, *J. Am. Chem. Soc.*, 2006, **128**, 7756–7757.
25 X. Li, M. Rui, J. Song, Z. Shen and H. Zeng, *Adv. Funct. Mater.*, 2015, **25**, 4929–4947.
26 S. Y. Lim, W. Shen and Z. Gao, *Chem. Soc. Rev.*, 2015, **44**, 362–381.
27 C. Hu, M. Li, J. Qiu and Y. Sun, *Chem. Soc. Rev.*, 2019, **48**, 2315–2337.
28 L. Wang, S. Zhu, H. Wang, S. Qu, Y. Zhang, J. Zhang, Q. Chen, H. Xu, W. Han, B. Yang and H. Sun, *ACS Nano*, 2014, **8**, 2541–2547.
29 Z. Kang and S. Lee, *Nanoscale*, 2019, **11**, 19214–19224.
30 F. Arcudi, L. Đorđević and M. Prato, *Acc. Chem. Res.*, 2019, **52**, 2070–2079.
31 F. Yan, Y. Jiang, X. Sun, J. Wei, L. Chen and Y. Zhang, *Nano Res.*, 2020, **13**, 52–60.
32 Z. Tian, X. Zhang, D. Li, D. Zhou, P. Jing, D. Shen, S. Qu, R. Zboril and A. L. Rogach, *Adv. Opt. Mater.*, 2017, **5**, 1700416.
33 X. Miao, D. Qu, D. Yang, B. Nie, Y. Zhao, H. Fan and Z. Sun, *Adv. Mater.*, 2018, **30**, 1704740.
34 J. Zhu, X. Bai, X. Chen, H. Shao, Y. Zhai, G. Pan, H. Zhang, E. V. Ushakova, Y. Zhang, H. Song and A. L. Rogach, *Adv. Opt. Mater.*, 2019, **7**, 1801599.
35 C. Shen, Q. Lou, C. Lv, J. Zang, S. Qu, L. Dong and C. Shan, *Adv. Sci.*, 2019, **6**, 1802331.
36 X. Song, Q. Guo, Z. Cai, J. Qiu and G. Dong, *Ceram. Int.*, 2019, **45**, 17387–17394.
37 Y. Yan, L. Xia and L. Ma, *RSC Adv.*, 2019, **9**, 24057–24065.
38 J. Zhu, X. Bai, J. Bai, G. Pan, Y. Zhu, Y. Zhai, H. Shao, X. Chen, B. Dong, H. Zhang and H. Song, *Nanotechnology*, 2018, **29**, 085705.
39 S. Lin, M. Chen, Z. Wang, Y. Zhang, R. Yuan, X. Liang, W. Xiang and Y. Zhou, *Chem. Eng. J.*, 2017, **324**, 194–202.
40 D. Chen, W. Wu, Y. Yuan, Y. Zhou, Z. Wan and P. Huang, *J. Mater. Chem. C*, 2016, **4**, 9027–9035.
41 A. Kundu, B. Park, J. Oh, K. V. Sankar, C. Ray, W. S. Kim and S. C. Jun, *Carbon*, 2020, **156**, 110–118.
42 Z. Xie, F. Wang and C. Liu, *Adv. Mater.*, 2012, **24**, 1716–1721.
43 S. K. Bhunia, S. Nandi, R. Shikler and R. Jelinek, *Nanoscale*, 2016, **8**, 3400–3406.
44 M. Sun, S. Qu, Z. Hao, W. Ji, P. Jing, H. Zhang, L. Zhang, J. Zhao and D. Shen, *Nanoscale*, 2014, **6**, 13076–13081.
45 D. Zhou, D. Li, P. Jing, Y. Zhai, D. Shen, S. Qu and A. L. Rogach, *Chem. Mater.*, 2017, **29**, 1779–1787.
46 J. Wang, F. Zhang, Y. Wang, Y. Yang and X. Liu, *Carbon*, 2018, **126**, 426–436.
47 D. Zhou, Y. Zhai, S. Qu, D. Li, P. Jing, W. Ji, D. Shen and A. L. Rogach, *Small*, 2017, **13**, 1602055.
48 J. He, Y. He, Y. Chen, B. Lei, J. Zhuang, Y. Xiao, Y. Liang, M. Zheng, H. Zhang and Y. Liu, *Small*, 2017, **13**, 1700075.
49 W. Li, S. Wu, X. Xu, J. Zhuang, H. Zhang, X. Zhang, C. Hu, B. Lei, C. F. Kaminski and Y. Liu, *Chem. Mater.*, 2019, **31**, 9887–9894.
50 L. Wang, X. Zhang, K. Yang, L. Wang and C. Lee, *Carbon*, 2020, **160**, 298–306.
51 S. Lu, L. Sui, J. Liu, S. Zhu, A. Chen, M. Jin and B. Yang, *Adv. Mater.*, 2017, **29**, 1603443.
52 H. Ding, S. Yu, J. Wei and H. Xiong, *ACS Nano*, 2016, **10**, 484–491.
53 L. Han, S. G. Liu, J. X. Dong, J. Y. Liang, L. J. Li, N. B. Li and H. Q. Luo, *J. Mater. Chem. C*, 2017, **5**, 10785–10793.
54 Z. Sheng, L. Shao, J. Chen, W. Bao, F. Wang and X. Xia, *ACS Nano*, 2011, **5**, 4350–4358.
55 D. Peng, X. Liu, M. Huang, D. Wang and R. Liu, *Dalton Trans.*, 2018, **47**, 5823–5830.
56 C. Shih, P. Chen, G. Lin, C. Wang and H. Chang, *ACS Nano*, 2015, **9**, 312–319.
57 C. Leu, S. Chen, F. Liu and C. Wu, *J. Mater. Chem.*, 2012, **22**, 2089–2098.
58 Y. Zhang, J. Feng, M. He, J. Jiang, T. Xu, L. Zhou, W. Chen, W. Xiang and X. Liang, *RSC Adv.*, 2017, **7**, 49542–49547.